ELSEVIER

Ceramics International 28 (2002) 699–704

CERAMICS INTERNATIONAL

www.elsevier.com/locate/ceramint

In situ formation of $LaAl_{11}O_{18}$ rodlike particles in ZTA ceramics and effect on the mechanical properties

R. Guo*, D. Guo, Y. Chen, Z. Yang, Q. Yuan

School of Materials Science and Engineering, Tianjin University, Tianjin 300072, PR China

Received 29 August 2001; received in revised form 17 December 2001; accepted 24 January 2002

Abstract

A small amount of sintering aids, which contain MgO, kaolin and La_2O_3, was introduced into ZTA ceramics to realize densification at low temperature and to obtain a fine-grained microstructure. On the base of this, different amounts of La_2O_3 were added and rodlike $LaAl_{11}O_{18}$ was formed in situ due to its anisotropic growth habit during sintering. The effects of sintering temperature and the amount of rodlike $LaAl_{11}O_{18}$ were investigated. It was shown that the mechanical properties of ZTA ceramics were improved by the $LaAl_{11}O_{18}$, with strength over 500 MPa and fracture toughness 7 $MPam^{1/2}$. As the $LaAl_{11}O_{18}$ amount increased, part of the t-ZrO_2 transformed to m-ZrO_2, which is revealed by the decrease in the peak intensity of X-ray diffraction pattern, and which brought about a reduction in hardness and Young's modulus. It is believed that crack bridging and crack deflection were major factors contributing to strengthening and toughening of the materials as revealed through the microstructural observations by SEM and TEM.

Keywords: C. Mechanical properties; ZTA ceramics; In situ formation; Rodlike particle; Microstructural toughening

1. Introduction

In the past decade, ceramists have been pursuing microstructural toughening through the use of a second phase with a high aspect ratio (whiskers, fibers and platelets). Whiskers or platelets can be incorporated into the matrix by mixing them mechanically with the raw powders before sintering [1–3]. However, the source of whisker or fiber for ceramic composites is limited and they are usually expensive. Furthermore, these composites are difficult to sinter to high density because of the constraint of the second-phase network, and they must be hot-pressed in most cases. So far it has been seldom reported to prepare composites by introducing rodlike particles directly due to difficulties in synthesizing them and their inhibitions to densification [4,5]. In the case of Al_2O_3/SiC-whisker composites, fracture toughness values higher than 6 $MPam^{1/2}$ have been reported [1]. Nevertheless, these improvements may occur at the expense of strength, when the second phase acts as a flaw initiation site. Theoretically, if the microstructural features are developed after densification is first completed, via in situ formation of a second phase, which has a highly anisotropic growth habit, a tough ceramic composite can be obtained without the sintering difficulty. Hori et al. [6] reported an in situ composite of TiO_2 matrix with dispersed corundum platelets whose anisotropic growth was promoted by sodium doping. Toughness up to 7 $MPam^{1/2}$ was obtained. In another case, in situ formation of elongated, rodlike grains of Si_3N_4 in Si_3N_4 sintered under a nitrogen-gas overpressure, resulted in self-reinforcement with an improved toughness in excess of 10 $MPam^{1/2}$, while strength remained quite good [7]. In both examples, high density could readily be achieved. Successful toughness enhancement was also reported for 3Y-TZP/mullite composites in which elongated mullite grains could be formed in situ [8].

Al_2O_3 is compatible with many aluminate compounds such as $LaAl_{11}O_{18}$, which has an anisotropic growth habit and is suitable for toughening reinforcement. By incorporating these rodlike particles into ZrO_2 transformation-toughened ceramics, favorable results have been reported [9–12]. In this paper, La_2O_3 is added to zirconia-toughened alumina (ZTA) and reacts with

* Corresponding author.
E-mail address: rsguo@tju.edu.cn (R. Guo).

0272-8842/02/$22.00
PII: S0272-8842(02)00031-7

Al_2O_3 to form in situ $LaAl_{11}O_{18}$ rodlike particles. These rodlike particles act as toughening agents to improve the mechanical properties of the composites, without any sintering problems due to their in situ formation during sintering. Because hardness and Young's modulus of aluminates are much lower than those of corundum, these properties of a composite decrease with increasing content of aluminates [11], giving rise to reduced constraint on the ZrO_2 from the surroundings. Therefore, ZrO_2 toughening eventually becomes less effective. Obviously, there is a compromise of aluminate content for gaining optimal mechanical properties. The present report focuses on the effects of sintering temperature and of the amount of incorporated aluminates on the mechanical properties of the composites and on the microstructural toughening mechanisms as observed by SEM and TEM.

2. Experiment

The composition of the ZTA ceramics is 15 vol.% 3Y-TZP/Al_2O_3. A small amount of sintering aid (0.5 wt.% MgO, 2 wt.% kaolin and 2 wt.% La_2O_3) (Table 1) was included to realize densification at lower temperatures. In addition, different amounts of La_2O_3 were added to form in situ rodlike $LaAl_{11}O_{18}$ (Table 2). With this objective, the $LaAlO_3$ powder was synthesized by calcining at 1100 °C for 1 h an equi-molar mixture of Al_2O_3 and La_2O_3 after homogeneously mixing by ball milling for 24 h. Composite powder of Al_2O_3, $LaAlO_3$, Y-TZP and sintering aid was ball-milled again with water for 24 h. After being dried and passed through a 40-mesh sieve to granulate, bars were obtained by pressing (100 MPa) and isostatic pressing (200 MPa), followed by sintering under different conditions. The sintered bars were ground before measurements of mechanical properties (3-point bending method). The size of test pieces was 2.5×3×30 mm and span 20 mm. The bars were pre-notched with the length 0.48–0.51 of height and the width 0.18∼0.2 mm before fracture toughness determination. The value of strength and fracture toughness was the average of 5 and 3 measurements, respectively. Bulk density was determined by the Archimedes method and relative density was calculated using the same theoretical density of 4.27 g/cm^3 for all materials simply. X-ray diffraction analysis was conducted for phase identification using CuK_α radiation and m-ZrO_2 fraction was calculated by the modified Garvie and Nicholson equation [13]

$$x_{m-ZrO_2} = \frac{I_{m(111)} + I_{m(11\,\bar{1})}}{I_{m(111)} + I_{m(11\,\bar{1})} + I_{t(111)}}.$$

where x_{m-ZrO_2} is the m-ZrO_2 fraction, $I_{t(111)}$, $I_{m(11\bar{1})}$ and $I_{m(111)}$ are the peak intensities corresponding to the tetragonal (111), monolithic ($11\bar{1}$) and monolithic (111) planes, respectively. Microstructure and crack propagation behavior observations were made using SEM and TEM.

3. Results and discussion

3.1. Sinterability and X-ray diffraction analysis

It was shown from the density measurements that a density higher than 98% of the theoretical one was obtained for all La_2O_3-containing materials after sintering at 1450 °C, revealing good sinterability. The main reason for this was attributed to the use of sintering aid. The density of Sample AL0 without La_2O_3 inclusion only reached 95.1%. It also demonstrated that the in situ formation of $LaAl_{11}O_{18}$ did not cause any sintering inhibition. With an increase of the sintering temperature, the densities decreased a little due to the formation of $LaAl_{11}O_{18}$, but were still over 96% after sintering at 1570 °C.

The phases identified by XRD for AL0, AL8 and AL32 samples sintered at 1450 °C are shown in Fig. 1. It can be seen from this pattern that $LaAl_{11}O_{18}$ formed apart from the α-Al_2O_3 and t-ZrO_2 main phases for the La_2O_3-containing samples. With increasing the

Table 1
Raw materials

α-Al_2O_3	SiO_2	Fe_2O_3	Na_2O	Other		Grain size	
98.9	0.085	0.026	0.5	0.485		<1μm	Shandong alumimum Co. Ltd, China
Y-TZP	SiO_2	Fe_2O_3	Na_2O	TiO_2	Cl^-	Grain size	
>99.8	<0.005	<0.005	<0.1	<0.001	<0.001	0.58μm	Farmeiya (Jiujiang) Advanced Material Co. Ltd, China
La_2O_3	Analytical grade						Shanghai Chemical Reagents Co. Ltd, China
MgO	Chemical grade						Shanghai Dunhuang Chemical Factory, China
Kaolin	Industrial grade						Suzhou, China

$LaAl_{11}O_{18}$ content, the intensity of the t-ZrO_2 peak decreased a little (Fig. 1), showing transformation from tetragonal symmetry to monoclinic one, which resulted from the reduction in Young's modulus, as mentioned above. Nonetheless, the content of m-ZrO_2 in both materials was quite low (Fig. 2), therefore, ZrO_2 toughening remained active.

3.2. Effects of the sintering temperature and $LaAl_{11}O_{18}$ content on bending strength of ZTA

Fig. 3 showed the variation of bending strength vs. the sintering temperature and $LaAl_{11}O_{18}$ content. It can be seen that maximum strength was obtained after sintering at 1400–1450 °C. When the sintering temperature is over 1500 °C, severe degradation of bending strength occurred. This might be attributed to over-sintering as revealed from the comparison between Fig. 4(a) and (b) which showed abnormal grain growth [14]. The in situ formation of rodlike $LaAl_{11}O_{18}$ phase happened after La_2O_3 was included in the composite [Fig. 4 (c)]. This elongated phase made a contribution to strengthening the materials compared with that without La_2O_3 inclusion [15]. The maximum strength occurred for a $LaAl_{11}O_{18}$ content of about 16–24%. It can be found that strength decreased when $LaAl_{11}O_{18}$ content was over 24%. This might be explained, as mentioned above, by the reduction in Young's modulus, which led to a partial transformation of t-ZrO_2 to m-ZrO_2 (see Fig. 2).

3.3. Effects of sintering temperature and $LaAl_{11}O_{18}$ content on fracture toughness of ZTA

Fig. 5(a) showed the relation between fracture toughness and sintering temperature for samples AL0, AL8 and AL32. A peak occurred for a sintering temperature of 1400 °C for each composition. The maximum value reached 7.2 $MPam^{1/2}$. The toughness value of AL8 sample is higher than that of AL32 at lower temperature, but lower at higher temperature. The reason for this will be discussed later.

An interesting change for the influence of $LaAl_{11}O_{18}$ content on fracture toughness was shown in Fig. 5(b) and (c). Fracture toughness increased with temperature when sintering temperature is below 1450 °C and $LaAl_{11}O_{18}$ content was high, revealing that toughening of rodlike $LaAl_{11}O_{18}$ functioned. Also, the maximum value of fracture toughness occurred at a sintering temperature of 1400–1450 °C. A change trend opposite to the above can be observed when sintering temperature is higher than 1500 °C. This phenomenon may be caused by the decrease in Young's modulus of the materials and by the partial transformation of t-ZrO_2 to m-ZrO_2, which will weaken the ZrO_2 toughening. This result was in good agreement with that of Ref. [11].

Table 2
Content of in situ formed $LaAl_{11}O_{18}$ in ZTA composites (wt.%)

Sample	AL0	AL8	AL16	AL24	AL32	AL40
$LaAl_{11}O_{18}$ content	0	8	16	24	32	40

3.4. Microstructure and toughening mechanism

Rodlike $LaAl_{11}O_{18}$ particles were observed only for samples with La_2O_3 inclusion. On increasing the amount of La_2O_3, the content of $LaAl_{11}O_{18}$ particles

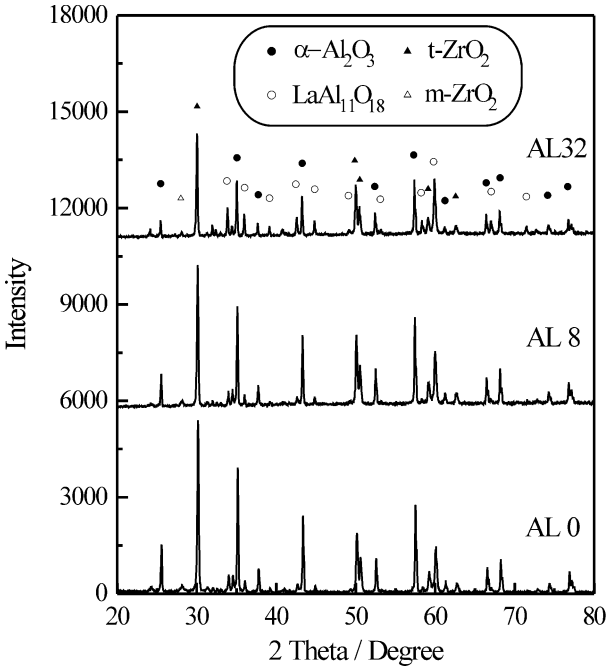

Fig. 1. X-ray diffraction patterns of AL0, AL8 and AL32 samples.

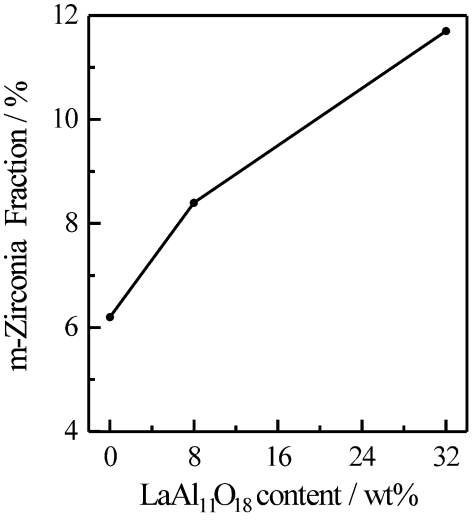

Fig. 2. m-ZrO_2 fraction vs. $LaAl_{11}O_{18}$ content.

increased as well. But their aspect ratio changed with sintering temperature. The growth rate of the diameter direction of the rodlike particles became greater than that of the length direction as sintering temperature increased, giving rise to a decrease in aspect ratio (Fig. 6). It is this phenomenon that caused the degradation of mechanical properties as sintering temperature increased.

As it is well known, different amounts of $LaAl_{11}O_{18}$ particles will produce different results for ZrO_2 toughening. This is only one aspect in question. The main contributions to strengthening and toughening of the

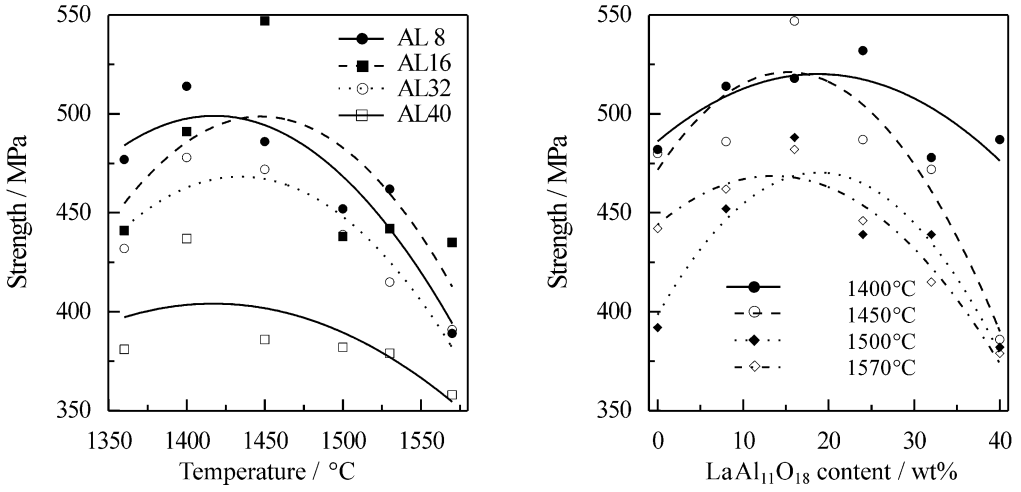

Fig. 3. Flexural strength vs. sintering temperature and $LaAl_{11}O_{18}$ content.

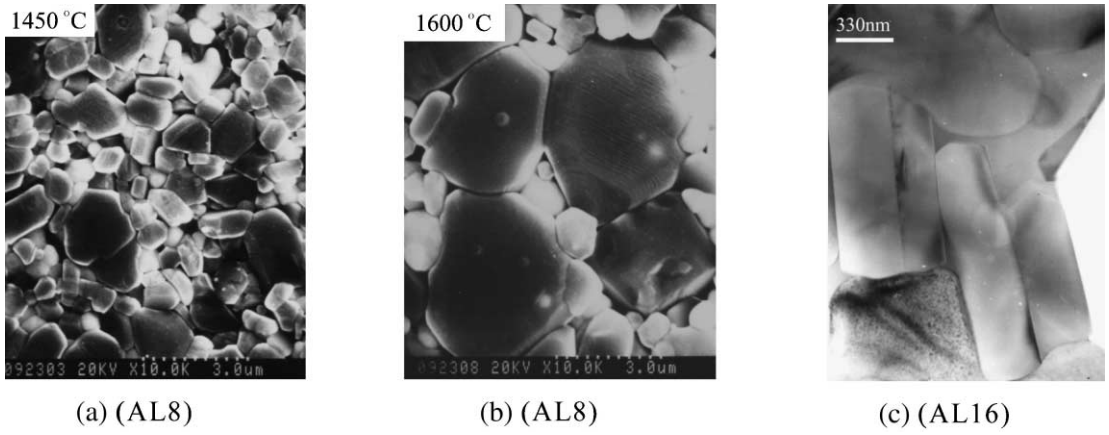

Fig. 4. SEM and TEM photographs of ZTA ceramics.

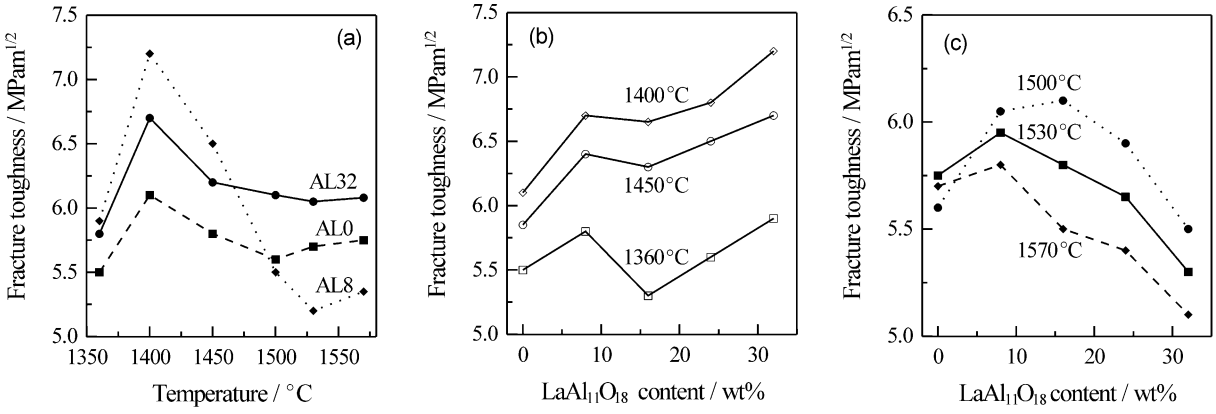

Fig. 5. Fracture toughness vs. sintering temperature and $LaAl_{11}O_{18}$ content.

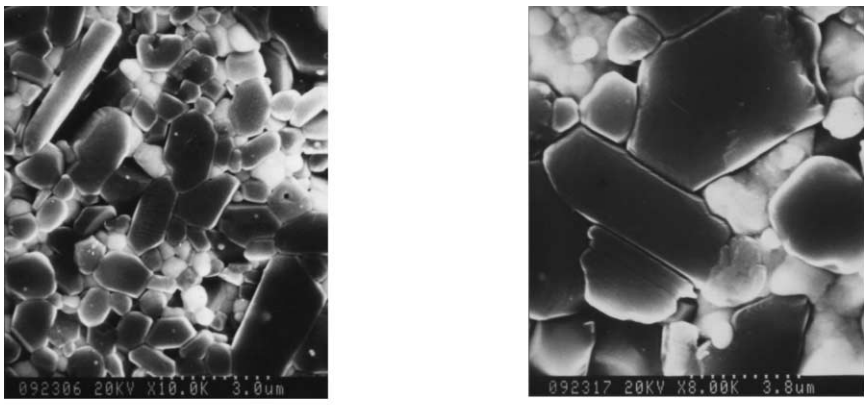

Fig. 6. SEM photographs of surface morphology of ZTA.

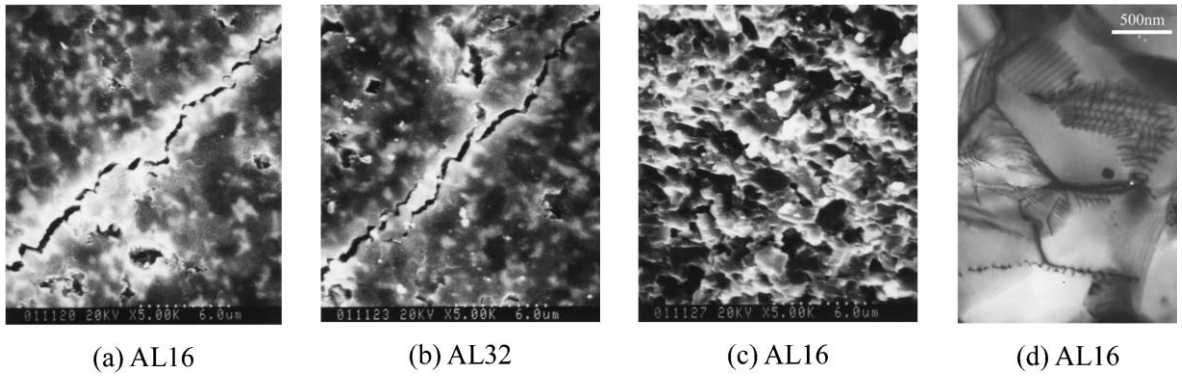

Fig. 7. Micrographs of ZTA ceramics. SEM photographs of crack propagation after indention (a and b), fracture section (c), TEM photograph (d).

material come from crack bridging of rodlike particles. As shown in Fig. 7(a) and (b), which were SEM photographs of propagation behavior of an indention crack, crack deflection and crack bridging can be clearly observed. It can also be seen that the fracture surface of a sample with higher mechanical properties was much rougher. There were some holes left in Fig. 7(c), which were produced by rodlike particle pullout. Transgranular fracture was predominant. In addition, a high density of dislocation was often observed for samples with the better mechanical properties, as shown in Fig. 7(d). These dislocations might make a contribution to strengthening the material. The similar phenomenon was once observed in the SiC_p-reinforced ZTM materials [16].

Toughening by whisker reinforcements can be expressed by the energy dissipation ΔJ as [17]

$$\Delta J = Vr\sigma_f^3/6E\tau$$

where V is the volume fraction of the whisker, r the whisker radius, σ_f the whisker fracture stress, E the Young's modulus of the whisker, and τ the interfacial friction between whisker and matrix. This result is based on the assumption that the interface toughness is low enough to allow the whisker to debond at the crack tip and that load is gradually transferred to the bridging whiskers in the wake by friction across the whisker interface. Evidently, high-aspect-ratio aluminate platelets partially fulfill the prerequisites for reinforcement by having a relatively large grain radius and a low elastic modulus. The interface toughness also seems sufficiently low, as suggested by the frequent observation of interface debonding. In our study, these demands were met quite well for the composites of ZTA/$LaAl_{11}O_{18}$, so the enhancements of the mechanical properties could be explained by this satisfactorily.

4. Summary

1. In situ formation of rodlike particle of $LaAl_{11}O_{18}$ did not affect sinterability of ZTA ceramics. In fact, this material can be sintered to high density at temperatures as low as 1400–1450 °C with the help of complex sintering aids. Bending strength over 500 MPa and fracture

toughness of 7 $MPam^{1/2}$ can be obtained at such low sintering temperatures.

2. Young's modulus of the composite material decreases as the amount of rodlike particles increases, resulting in weakening the constraint of ZrO_2 suffered from the surroundings and transformation from tetragonal symmetry to monoclinic.
3. When the materials were sintered at different temperatures, high rodlike particle content led to decrease in strength, but fracture toughness increased at low sintering temperature and decreased at high sintering temperature.
4. It was found from the observation of the microstructure that crack bridging and crack deflection were the main strengthening and toughening mechanism contributing to the improvement of mechanical properties.

References

[1] G.C. Wei, P.F. Becher, Development of SiC-whisker-reinforced ceramics, Am. Ceram. Soc. Bull. 64 (1985) 298–304.
[2] P.F. Becher, C.H. Hsueh, P. Angelini, et al., Toughening behavior in whisker-reinforced ceramic matrix composites, J. Am. Ceram. Soc. 71 (1988) 1050–1061.
[3] G.H. Campbell, M. Ruhle, B.J. Dalgleish, et al., Whisker toughening: a comparison between aluminum oxide and silicon nitride toughened with silicon carbide, J. Am. Ceram. Soc. 73 (1990) 521–530.
[4] H. Sakai, K. Matsuhiro, Y. Furuse, Mechanical properties of SiC platelet reinforced ceramic composites, in: D. Sacks (Ed.), Ceramic Transactions, Vol. 19, Advanced Composite Material, American Ceramic Society, Westerville, OH, 1991, pp. 765–771.
[5] T. Claussen, N. Claussen, Processing routes and microstructure of ceramic matrix/platelet composites, in: R. Carlsson, T. Johansson, L. Kahlman (Eds.), 4th International Symposium on Ceramic Materials and Components for Engines, Elsevier Applied Science, London, UK, 1992, pp. 715–725.
[6] S. Hori, H. Kaji, M. Yoshimura, et al., Deflection-toughened corundum-rutile composites, Mater. Res. Soc. Proc. 78 (1987) 283–288.
[7] E. Tani, S. Umebayyashi, K. Kishi, et al., Gas-pressure sintering of Si_3N_4 with concurrent addition of Al_2O_3 and 5 wt.% rare-earth oxide: high fracture toughness Si_3N_4 with fiber-like structure, Am. Ceram. Soc. Bull. 65 (1986) 1311–1315.
[8] K. Okada, N. Otsuka, R.J. Brook, et al., Microstructure and fracture toughness of yttria-doped tetragonal zirconia polycrystal/mullite composites prepared by an in situ method, J. Am. Ceram. Soc. 72 (1989) 2369–2372.
[9] K. Tsukuma, T. Takahata, Mechanical property and microstructure of TZP and TZP/Al_2O_3 composites, Mater. Res. Soc. Symp. Proc. 78 (1987) 123–135.
[10] R.A. Culter, R.J. Nayhew, K.M. Prettyman, et al., High toughness Ce-TZP/Al_2O_3 ceramics with improved hardness and strength, J. Am. Ceram. Soc. 74 (1991) 179–186.
[11] P.-L. Chen, I.-W. Chen, In-situ alumina/aluminate platelet composites, J. Am. Ceram. Soc. 75 (1992) 2610–2612.
[12] M. Yasuoka, K. Hirao, M.E. Brito, et al., High-strength and high-fracture-toughness ceramics in the $Al_2O_3/LaAl_{11}O_{18}$ system, J. Am. Ceram. Soc. 78 (1996) 1853–1856.
[13] R.C. Garvie, P.S. Nicholson, Phase analysis in zirconia system, J. Am. Ceram. Soc. 55 (1972) 303–305.
[14] R. Guo, Z. Yang, Q. Yuan, et al., Influences of complex sintering aids on sinterability of ZTA ceramics, J. Chinese Ceram. Soc. 27 (1999) 258–263.
[15] R. Guo, Y. Chen, Z. Yang, et al., Improvement of mechanical property of alumina-based ceramics by taking advantage of complex sintering aids, J. Ceramics 20 (1999) 9–12.
[16] R. Guo, Z. He, Z. Yang, et al., Controlling the flaw size and mechanical properties of ZTM/SiCp composites, J. Eur. Ceram. Soc. 16 (1996) 1345–1349.
[17] P.F. Becher, Microstructural design of toughened ceramics, J. Am. Ceram. Soc. 74 (1991) 179–186.